JOURNAL OF VIROLOGY, Dec. 1995, p. 8070–8075 Vol. 69, No. 12
0022-538X/95/$04.00+0

Characterization of a Neurologic Disease Induced by a Polytropic Murine Retrovirus: Evidence for Differential Targeting of Ecotropic and Polytropic Viruses in the Brain

JOHN L. PORTIS,* STEFANIE CZUB,† SHELLY ROBERTSON, FRANK MCATEE, AND BRUCE CHESEBRO

Laboratory of Persistent Viral Diseases, Rocky Mountain Laboratories, National Institute of Allergy and Infectious Diseases, Hamilton, Montana 59840

Received 29 June 1995/Accepted 25 August 1995

A variety of ecotropic murine leukemia viruses cause neurodegenerative disease. We describe here the clinical and histopathological features of a neurologic disease induced by a polytropic murine leukemia virus, FMCF98. Clinical disease was dominated by hyperexcitability and ataxia, and the histopathology was characterized primarily by astrocytosis and astrocytic degeneration. The viral envelope gene harbored the determinants of neurovirulence, since the chimeric virus Fr98^E, which contained the envelope gene of FMCF98 on a background of the nonneurovirulent virus FB29, caused a similar disease. The disease caused by Fr98^E differed from that induced by the coisogenic neurovirulent ecotropic virus FrCas^E in clinical presentation, histopathology, and distribution of virus in the central nervous system. Since Fr98^E contains a polytropic envelope gene and FrCas^E contains an ecotropic envelope gene, these phenotypic differences appeared to be determined by envelope sequences and may reflect differences in virus receptor usage in the central nervous system.

Several ecotropic murine retroviruses induce spongiform neurodegenerative disease manifested clinically by tremor and paralysis, usually of the hind limbs (26, 37). Included among this group are two temperature-sensitive mutants of Moloney murine leukemia virus (MuLV) (3, 37), a variant of Friend MuLV (17, 19), and CasBr, a virus recovered from wild mice (12). Mapping studies have indicated that the primary determinants of neurovirulence reside within the respective envelope genes (10, 24, 35). However, the role of the viral envelope gene in disease pathogenesis is not understood.

These neurovirulent murine retroviruses have a number of qualities in common. They all belong to the ecotropic host range group, indicating that they use a common receptor to infect the host cell. They all induce a form of neurodegenerative disease which is manifested by tremulous paralysis (26), noninflammatory spongiform degeneration (21, 25, 38), and lesion distribution in motor nuclei as well as major sensorimotor relay centers of the brain and spinal cord (4, 9, 38). The distribution of virus within the central nervous system exhibits both similarities and differences. For the temperature-sensitive Moloney and wild-mouse CasBr isolates, viral gene products have been detected in a wide variety of cell types both in regions exhibiting neuronal cytopathology and in apparently unaffected areas (1, 2, 20, 21). The infected cells include endothelial cells and pericytes as well as neurons and glia, although spongiform lesions appear associated primarily with infection of microglial cells (2, 16, 21, 23). For the Friend MuLV variant PVC211, the distribution of virus appears to be quite different, having been identified only within the vascular endothelial cells (17). The mechanism of neurodegeneration in each of these diseases seems to be indirect, since the neurons exhibiting cytopathology appear not to be infected.

We have described a polytropic murine retrovirus, FMCF98 (formerly called F-MCF98D [7]), which also causes neurologic disease (5) but enters the host cell by a receptor different from that utilized by the ecotropic viruses (7, 29). We describe the initial characterization of this disease, which exhibits unique clinical, histopathological, and virologic features, all of which are determined by the viral envelope gene.

Characterization of the clinical disease induced by FMCF98. FMCF98 was originally isolated from the spleen of a BALB/c mouse infected with Friend MuLV (7), and its characteristics have been determined in vivo with virus biologically cloned by limiting dilution (5). Using a previously described strategy (34), the viral genome was molecularly cloned from unintegrated circular DNA at the unique *Kpn*I site in the R region of the viral long terminal repeat. A clone, designated 18-4, was transfected into NIH 3T3 cells, and, after spread of virus throughout the culture, viral stocks were made from supernatant fluid. To test for pathogenicity in vivo, 10^4 focus-forming units of virus (33) was inoculated intraperitoneally into neonatal IRW mice (27) $\leq$48 h after birth. The first signs of neurologic disease consisted of hyperactivity with an accentuated arousal response to noise. At this time some mice exhibited a tendency to run off the edge of the table without hesitation, suggesting a disturbance of the visual pathway. These signs were followed by ataxia, which was manifested by falling to either side when attempting to climb up the walls of the cage. These signs appeared to be a consequence of imbalance; however, some component of hind-limb weakness may also have been present. During this period the mice continued to groom themselves and their coats appeared smooth and shiny. As ataxia became more severe, mice were found lying immobile, often on their sides. When aroused, they were ambulatory and able to use both forelimbs and hind limbs, but they had a wobbly gait. When the animals were handled, a fine tremor was noted. As the disease progressed, mice were found lying im-

* Corresponding author. Phone: (406) 363-9339. Fax: (406) 363-9204.

† Present address: Pathologisches Institut, Universität Würzburg, Würzburg, Germany.

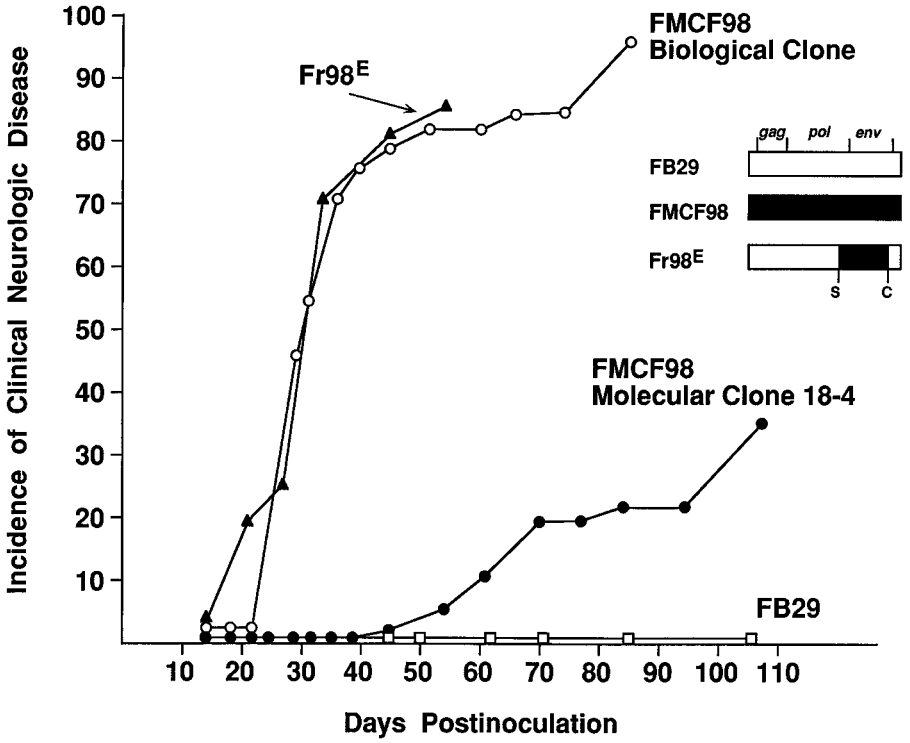

FIG. 1. Cumulative incidence of clinical disease as a function of time after inoculation. Neonatal IRW mice were inoculated with virus stocks of the biological clone of FMCF98 (n = 38), the molecular FMCF98 clone 18-4 (n = 59), the chimeric virus Fr98^E (n = 21), and the Friend MuLV parent of Fr98^E, FB29 (n = 15). Mice were considered clinically affected when they exhibited the first signs of clinical disease. Comparison of FB29 and Fr98^E indicated that the 3′ *pol* and envelope genes of FMCF98 harbored the neurovirulence determinant(s). Comparison of clone 18-4 with Fr98^E indicated that nonenvelope sequences from FB29 accelerated the onset of clinical disease. The genomes are represented by bars at the upper right. S, *Sph*I; C, *Cla*I.

mobile and were unarousable. Prior to terminal stages of dehydration, the mice were euthanized.

For the biological clone of FMCF98, the incubation period to onset of disease was relatively short (30 to 80 days) and the incidence of disease was 100% (Fig. 1). In contrast, the induction of disease by the molecular clone 18-4 was inconsistent. The first signs of clinical disease appeared 55 to 105 days postinoculation (Fig. 1), and the incidence of disease over this period rarely exceeded 40%. This difference in neuropathogenicity of the biological and molecular clones has been observed with CasBr as well (26, 27) and is likely a consequence of sequence heterogeneity in the original biological isolate. In the case of CasBr, we were able to dramatically accelerate the disease by introducing its envelope gene (bounded on the 5′ side by an *Sph*I site and on the 3′ side by a *Cla*I site) into the genome of the nonneurovirulent Friend MuLV, strain FB29 (34). We therefore constructed a similar chimeric virus, Fr98^E, by introducing the *Sph*I-*Cla*I fragment from FMCF98 into FB29 (8).

Like its polytropic parent, Fr98^E has a polytropic host range and exhibits the viral interference pattern of a polytropic virus (8). This virus induced a clinical picture which was indistinguishable from that caused by both the molecular and the biological clones of FMCF98 (Fig. 1). The incubation period of 20 to 50 days for Fr98^E was similar to that of the biological clone of FMCF98 and much shorter than that of the molecular clone 18-4. The incidence of disease induced by Fr98^E over an observation period of 100 days was 90 to 100%. FB29 did not cause neurologic disease (Fig. 1) (27). These results indicate that important determinants of neuropathogenicity are located in the envelope gene of FMCF98. Disease acceleration by FB29 sequences is consistent with the results of previous studies with the neurovirulent ecotropic virus CasBr (28) for which we mapped the relevant FB29 sequences to a segment within the 5′ leader sequence of the viral genome, immediately upstream of the start site of pr65^{gag}, the precursor of the virion core proteins.

Pathological features of the neurologic disease caused by Fr98^E. Since the disease induced by Fr98^E was consistent and predictable, pathological studies were carried out on 15 clinically affected mice which had been neonatally inoculated (intraperitoneally) with this virus. Despite the rather dramatic nature of the clinical disease, light-microscopic examination of the brain and spinal cord revealed only subtle changes. These consisted of isolated vacuoles most frequently observed in the lateral cerebellar nucleus (dentate nucleus) (Fig. 2A). These vacuoles were sometimes associated with increased numbers of glial cells with dark staining and often elongated nuclei (Fig. 2A, arrow and inset), resembling activated microglial cells (30). Vacuoles were observed primarily in the neuropil and did not involve neuron cell bodies. Occasionally, vacuoles contained eosinophilic amorphous material and sometimes also contained a single nucleus resembling that of an astrocyte (Fig. 2B, arrow). Sparse vacuoles were observed in white-matter tracts, particularly the cerebellar peduncles (not shown) as well as focally in the cerebellar cortex (Fig. 2C). Occasionally, vacuoles were also observed in the internal capsule in the more rostral levels of the brain stem (not shown). However, other than the finding of scattered vacuoles in the lateral cerebellar nucleus, spongiform degeneration was an inconsistent finding and required careful comparison with age-matched uninoculated controls.

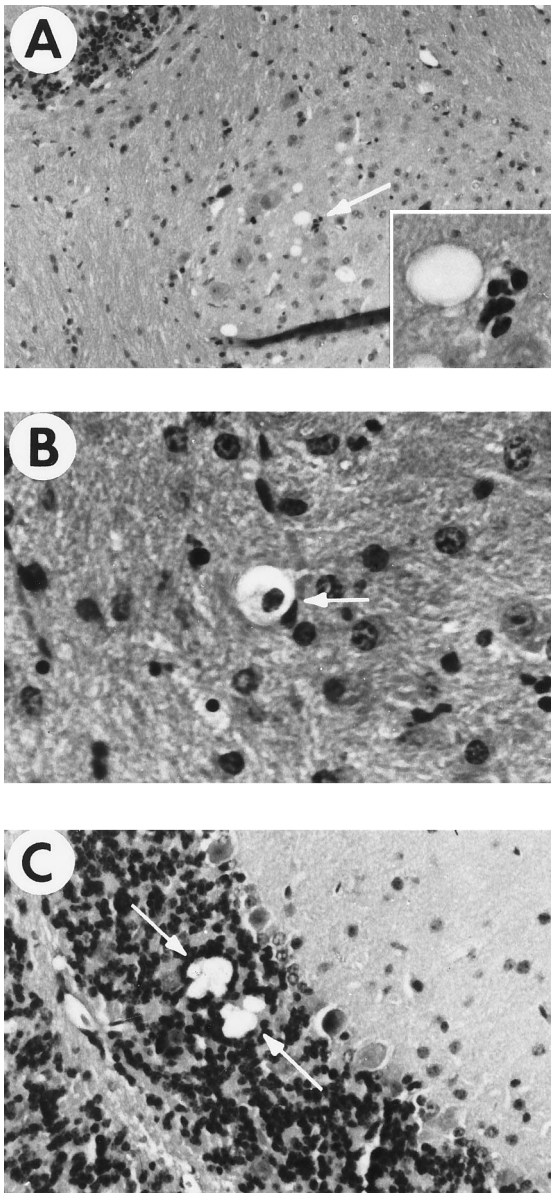

FIG. 2. Lesions induced by Fr98^E. Scattered vacuoles were consistently observed in the lateral cerebellar nucleus (dentate nucleus), and, occasionally, collections of glial cells resembling microglia were also observed (A, arrow and inset). Vacuoles sometimes contained a nucleus which resembled that of an astrocyte (B, arrow). Sparse vacuoles were also seen in the cerebellar cortex (C, arrows). Paraffin sections were stained with hematoxylin and eosin as described previously (9). Magnification, ×100.

Associated with this rather mild vacuolar change was an intense glial reaction characterized by high-level expression of the astrocyte marker glial fibrillary acidic protein (GFAP) (Fig. 3B). Except for the peripheral glial limitans of the brain stem, GFAP expression was essentially undetectable in uninoculated controls (Fig. 3A) (11). It is particularly noteworthy that some of the vacuoles contained amorphous material which stained with the anti-GFAP antiserum (Fig. 3C and D, arrows). This observation and the finding that some vacuoles contained astrocytic nuclei suggested that at least a component of the vacuolar degeneration consisted of degenerating astrocytes. Neither Luxol fast blue nor immunostaining for myelin basic protein revealed evidence of demyelination in this disease. Clinically affected mice which had been inoculated with the biological clone of FMCF98 (five mice) and the molecular clone 18-4 (six mice) were also examined histologically, and the lesions were indistinguishable both in degree and in distribution from the lesions in Fr98^E-inoculated mice.

The relationship between histopathology and the clinical signs was difficult to assess in this disease. Ataxia, which was a prominent clinical feature, was consistent with the observed involvement of the cerebellar cortex and deep cerebellar nuclei. On the other hand, a more general sensory deficit, suggested by the apparent visual disturbance in some mice, could not be excluded. In general, there was a striking contrast between the severity of the clinical manifestations and the paucity of vacuolar degeneration in this disease.

Virus localization in the brain. We examined the distribution of Fr98^E using biotinylated anti-SU (gp70) monoclonal antibody 720 (31), which reacts with Fr98^E but not with endogenous viruses. Viral antigen was restricted to white-matter tracts of the cerebellum and cerebellar peduncles (Fig. 4A), internal capsule, and corpus callosum (not shown). The infected cells were of two morphological types, endothelial cells associated with small vessels (Fig. 4B, arrows) and cells with highly ramified processes and compact cell bodies (Fig. 4C). Occasionally, clusters of these cells resembling the cell clusters in hematoxylin- and eosin-stained sections (Fig. 2A) were seen (Fig. 4D). The location of these virus-positive cells in the white matter identifies them as glial cells, although they were not further characterized with cell-type-specific markers.

Contrasting the diseases caused by Fr98^E and the neurovirulent ecotropic virus FrCas^E. Fr98^E is coisogenic with the chimeric ecotropic virus FrCas^E (8). Both viruses carry the long terminal repeat and the *gag* and 5′ *pol* genes of FB29 but differ in their 3′ *pol* and *env* genes (Fig. 5A). FrCas^E, which contains the *env* gene of CasBr, causes a paralytic disease affecting both forelimbs and hind limbs with an incubation period of only 15 to 16 days. Thus, the incubation period is shorter than that of Fr98^E, and the clinical disease is qualitatively different (paralysis versus ataxia). Unlike Fr98^E, FrCas^E causes extensive spongiform degeneration in the spinal cord, brain stem, and cerebral cortex (9, 21, 27). Both viruses induce gliosis (9). Thus, the neurologic diseases induced by these two viruses differ both kinetically and qualitatively, and these differences appeared to be determined by their respective envelope genes. It was therefore of interest to compare the infections of the brain by these two viruses.

Virus in the brain was quantified by Western blot (immunoblot) analysis (22). Whole brains were homogenized in 0.01 M Tris-HCl–0.15 M NaCl–0.001 M EDTA containing 0.5% Nonidet P-40. Insoluble material including nuclei was pelleted, and the supernatant was boiled after addition of sodium dodecyl sulfate and 2-mercaptoethanol (final concentrations, 2 and 5%, respectively). Protein was separated in 9% polyacrylamide gels, blotted onto Immobilon P membranes (Millipore), and detected with rabbit anti-p30 antiserum and the ECL system (Amersham) as previously described (9). Three clinically affected mice were analyzed per group, 16 days postinoculation for FrCas^E and 22 days postinoculation for Fr98^E. In both groups abundant viral protein was detected, although there was consistently three- to fourfold more p30 in the brains of FrCas^E-inoculated mice than in the brains of Fr98^E-inoculated mice (Fig. 5B).

FrCas^E has been shown to infect a variety of cell types throughout the brain including endothelial cells and pericytes of the vasculature, glial cells in both grey matter and white matter, and certain populations of neurons which divide postnatally (21). Most of these cell types also appeared to be

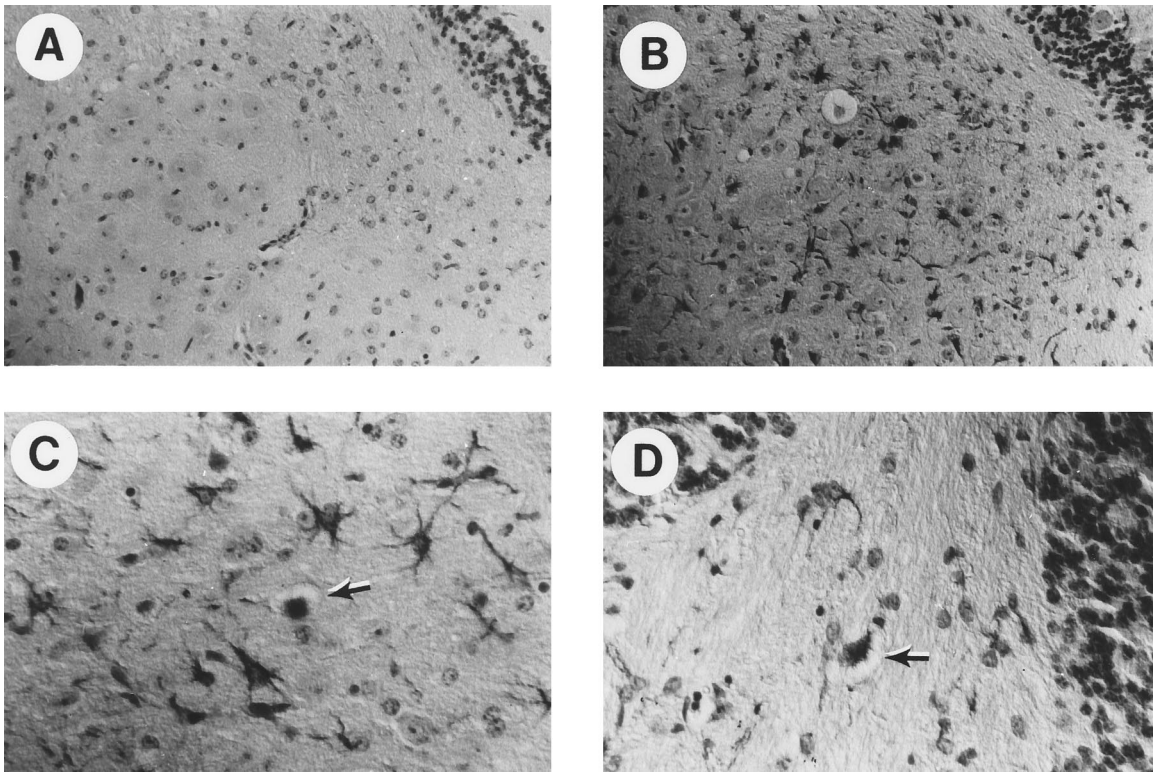

FIG. 3. Reactive gliosis was a consistent observation with mice inoculated with $Fr98^E$. Shown here are paraffin sections of the lateral cerebellar nucleus stained for GFAP as previously described (9). Although no staining was observed for the uninoculated control (A), abundant GFAP-positive astrocytes were noted for the infected mouse (B). High-power views of the lateral cerebellar nucleus (C) and cerebellar white matter (D) stained for GFAP showed vacuoles containing GFAP-positive amorphous material (arrows). Sections were lightly counterstained with Mayer's hematoxylin and viewed by differential interference microscopy. Magnification, ×200 (A and B) or ×400 (C and D).

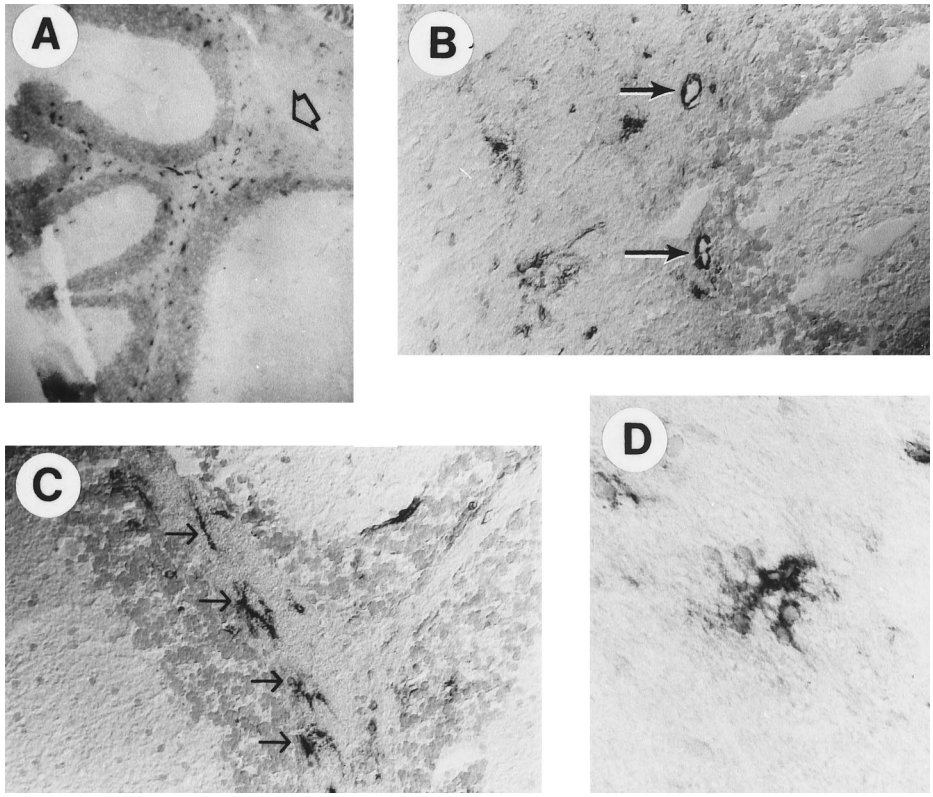

FIG. 4. Localization of viral antigen in an $Fr98^E$-infected mouse. Frozen sections of cerebellar white matter were stained with biotinylated monoclonal antibody 720 (31) and horseradish peroxidase-avidin developed with substrate AEC as previously described (9). A low-power sagittal view of the cerebellum (A) revealed virus-infected cells (darkly staining structures) in the white matter (arrow). The infected cells consisted of cells lining blood vessels (B, arrows) as well as highly arborized glial elements (C, arrows). The infected glial cells were occasionally found in clusters (D). Sections were lightly counterstained with Mayer's hematoxylin. For panels B to D, differential interference microscopy was used. Magnification, ×20 (A), ×100 (B and C), or ×300 (D).

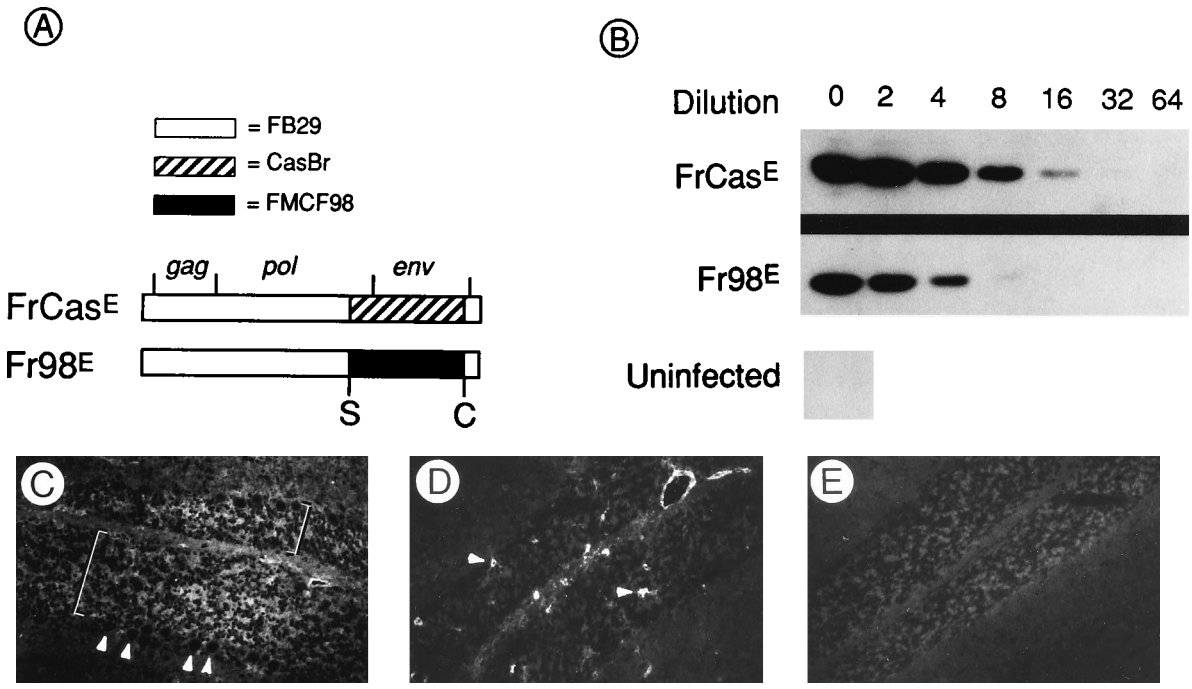

FIG. 5. Quantitative and qualitative differences between infections of the brain by $FrCas^E$ and $Fr98^E$. (A) Schematic of the structure of the ecotropic virus $FrCas^E$ and the polytropic virus $Fr98^E$, which differ only in sequences bounded by an *Sph*I (S) site in the 3′ *pol* gene and a *Cla*I (C) site at the 3′ end of the *env* gene. (B) Western blot analysis of p30 capsid protein expressed in brains of $FrCas^E$- and $Fr98^E$-inoculated mice 16 and 22 days postinoculation, respectively. Both mice exhibited severe clinical signs of neurologic disease. The uninfected control was 18 days of age. The level of $FrCas^E$ p30 in the brain was consistently three- to fourfold higher than that of $Fr98^E$ (three mice per group). (C to E) Frozen sections of the cerebellar cortices of mice neonatally inoculated with $FrCas^E$ (16 days postinoculation) or $Fr98^E$ (22 days postinoculation) or left uninoculated (18 days of age), respectively. Frozen cerebellar cortex sections were stained for viral envelope glycoprotein with a polyclonal goat antiserum kindly provided by Roland Friedrich, Institute of Medical Virology, Giessen, Germany), followed by fluorescein isothiocyanate donkey anti-goat immunoglobulin (ICN Biomedicals Inc.). Note the intense staining of the small, closely packed neurons in the granule layer (brackets) in the $FrCas^E$-inoculated mouse and the sparing of Purkinje neurons (arrowheads). In contrast, the small granule neurons in the $Fr98^E$-inoculated mouse were not stained (D). However, other cells in the granule layer (D, arrowheads), as well as vascular elements (upper right in panel D), were infected by $Fr98^E$. Magnification, ×66.

infected by $Fr98^E$. However, examination of the cerebellar cortex revealed that $Fr98^E$ failed to infect granule neurons (Fig. 5D), one of the populations of neurons which divide postnatally and are extensively infected by $FrCas^E$ (9, 21) (Fig. 5C). For $FrCas^E$ the infection of granule neurons appears to be an epiphenomenon, not directly involved in lesion induction (23). Nevertheless, the difference in infection of granule neurons by these two viruses demonstrates that the envelope gene can influence virus targeting in the central nervous system. Since $FrCas^E$, an ecotropic virus, and $Fr98^E$, a polytropic virus, use different receptors to enter the host cell, it is likely that these receptors are differentially expressed in some cell types in the brain.

This polytropic MuLV-induced neurologic disease presents two perplexing, though perhaps interrelated, questions: (i) what is the nature of the insult which underlies the severe clinical disease and (ii) what is the stimulus of the intense astrocytosis? The former question is a familiar one in AIDS dementia, in which there may be a paucity of virus-infected cells in the brain (18, 36) and in which there is a lack of reproducible pathological correlates of the often severe clinical disease (15). This has suggested that neurotoxic or perhaps gliotoxic products of virus-infected cells may, in part, be responsible for the clinical disease (14). In $Fr98^E$-infected mice, the most consistent pathological finding was an intense astrogliosis associated with focal astrocytic degeneration. Astrocytosis is generally thought to occur in response to neuronal injury (11). However, neuronal cytopathology, at least demonstrable by standard histopathological techniques, appeared to be minimal in this disease. Virus-infected cells were restricted primarily to white-matter tracts, yet the gliosis was widespread in both grey matter and white matter, suggesting that the astrogliosis was induced by diffusible factors. Astrocytes are known to be activated by cytokines such as interleukin-1 (13) and interleukin-6 (32). Furthermore, overproduction of an interleukin-6 transgene in the brain induced a neurologic disease reminiscent both clinically and pathologically of the disease described herein (6). It is, therefore, possible that both the neuronal dysfunction and the astrogliosis in this disease may be mediated by cytokines expressed in response to the virus infection.

REFERENCES

1. **Baszler, T. V., H. E. Whiteley, and J. F. Zachary.** 1992. Ocular infection with a murine neurovirulent retrovirus does not cause retinal degeneration. Invest. Ophthalmol. Vis. Sci. **33:**384–389.
2. **Baszler, T. V., and J. F. Zachary.** 1991. Murine retroviral neurovirulence correlates with an enhanced ability of virus to infect selectively, replicate in, and activate resident microglial cells. Am. J. Pathol. **138:**655–671.
3. **Bilello, J. A., O. M. Pitts, and P. M. Hoffman.** 1986. Characterization of a progressive neurodegenerative disease induced by a temperature-sensitive Moloney murine leukemia virus infection. J. Virol. **59:**234–241.
4. **Brooks, B. R., J. R. Swarz, and R. T. Johnson.** 1980. Spongiform polioencephalomyelopathy caused by a murine retrovirus. I. Pathogenesis of infection in newborn mice. Lab. Invest. **43:**480–486.
5. **Buller, R. S., K. Wehrly, J. L. Portis, and B. Chesebro.** 1990. Host genes conferring resistance to a central nervous system disease induced by a polytropic recombinant Friend murine retrovirus. J. Virol. **64:**493–498.
6. **Campbell, I. L., C. R. Abraham, E. Masliah, P. Kemper, J. D. Inglis, M. B. A. Oldstone, and L. Mucke.** 1993. Neurologic disease induced in transgenic mice by cerebral overexpression of interleukin 6. Proc. Natl. Acad. Sci. USA **90:**10061–10065.

7. **Chesebro, B., and K. Wehrly.** 1985. Different murine cell lines manifest unique patterns of interference to superinfection by murine leukemia viruses. Virology **141:**119–129.
8. **Czub, M., F. J. McAtee, S. Czub, W. P. Lynch, and J. L. Portis.** 1995. Prevention of retrovirus-induced neurological disease by infection with a nonneuropathogenic retrovirus. Virology **206:**372–380.
9. **Czub, S., W. P. Lynch, M. Czub, and J. L. Portis.** 1994. Kinetic analysis of spongiform neurodegenerative disease induced by a highly virulent murine retrovirus. Lab. Invest. **70:**711–723.
10. **DesGroseillers, L., M. Barrette, and P. Jolicoeur.** 1984. Physical mapping of the paralysis-inducing determinant of a wild mouse ecotropic neurotropic virus. J. Virol. **52:**356–363.
11. **Eddleston, M., and L. Mucke.** 1993. Molecular profile of reactive astrocytes—implications for their role in neurologic disease. Neuroscience **54:**15–36.
12. **Gardner, M. B., B. E. Henderson, J. E. Officer, R. W. Rongey, J. C. Parker, C. Oliver, J. D. Estes, and R. J. Huebner.** 1973. A spontaneous lower motor neuron disease apparently caused by indigenous type-C RNA virus in wild mice. J. Natl. Cancer Inst. **51:**1243–1254.
13. **Giulian, D., J. Li, L. Xia, J. George, and P. A. Rutecki.** 1994. The impact of microglial-derived cytokines upon gliosis in the CNS. Dev. Neurosci. **16:**128–136.
14. **Giulian, D., K. Vaca, and C. Noonan.** 1990. Secretion of neurotoxins by mononuclear phagocytes infected with HIV-1. Science **250:**1593–1596.
15. **Glass, J. D., S. L. Wesselingh, O. A. Selnes, and J. C. McArthur.** 1993. Clinical-neuropathologic correlation in HIV-associated dementia. Neurology **43:**2230–2237.
16. **Gravel, C., D. G. Kay, and P. Jolicoeur.** 1993. Identification of the infected target cell type in spongiform myeloencephalopathy induced by the neurotropic Cas-Br-E murine leukemia virus. J. Virol. **67:**6648–6658.
17. **Hoffman, P. M., E. F. Cimino, D. S. Robbins, R. D. Broadwell, J. M. Powers, and S. K. Ruscetti.** 1992. Cellular tropism and localization in the rodent nervous system of a neuropathogenic variant of Friend murine leukemia virus. Lab. Invest. **67:**314–321.
18. **Johnson, R. T., J. C. McArthur, and O. Narayan.** 1988. The neurobiology of human immunodeficiency virus infections. FASEB J. **2:**2970–2981.
19. **Kai, K., and T. Furuta.** 1984. Isolation of paralysis-inducing murine leukemia viruses from Friend virus passaged in rats. J. Virol. **50:**970–973.
20. **Kay, D. G., C. Gravel, Y. Robitaille, and P. Jolicoeur.** 1991. Retrovirus-induced spongiform myeloencephalopathy in mice: regional distribution of infected target cells and neuronal loss occurring in the absence of viral expression in neurons. Proc. Natl. Acad. Sci. USA **88:**1281–1285.
21. **Lynch, W. P., S. Czub, F. J. McAtee, S. F. Hayes, and J. L. Portis.** 1991. Murine retrovirus-induced spongiform encephalopathy: productive infection of microglia and cerebellar neurons in accelerated CNS disease. Neuron **7:**365–379.
22. **Lynch, W. P., and J. L. Portis.** 1993. Murine retrovirus-induced spongiform encephalopathy: disease expression is dependent on postnatal development of the central nervous system. J. Virol. **67:**2601–2610.
23. **Lynch, W. P., S. J. Robertson, and J. L. Portis.** 1995. Induction of focal spongiform neurodegeneration in developmentally restricted mice by implantation of murine retrovirus-infected microglia. J. Virol. **69:**1408–1419.
24. **Masuda, M., P. M. Hoffman, and S. K. Ruscetti.** 1993. Viral determinants that control the neuropathogenicity of PVC-211 murine leukemia virus in vivo determine brain capillary endothelial cell tropism of the virus in vitro. J. Virol. **67:**4580–4587.
25. **Oldstone, M. B. A., P. W. Lampert, S. Lee, and F. J. Dixon.** 1977. Pathogenesis of the slow disease of the central nervous system associated with WM 1504 E virus. I. Relationship of strain susceptibility and replication to disease. Am. J. Pathol. **88:**193–212.
26. **Portis, J. L.** 1990. Wild mouse retrovirus: pathogenesis. Curr. Top. Microbiol. Immunol. **160:**11–27.
27. **Portis, J. L., S. Czub, C. F. Garon, and F. J. McAtee.** 1990. Neurodegenerative disease induced by the wild mouse ecotropic retrovirus is markedly accelerated by long terminal repeat and *gag-pol* sequences from nondefective Friend murine leukemia virus. J. Virol. **64:**1648–1656.
28. **Portis, J. L., G. J. Spangrude, and F. J. McAtee.** 1994. Identification of a sequence in the unique 5′ open reading frame of the gene encoding glycosylated Gag which influences the incubation period of neurodegenerative disease induced by a murine retrovirus. J. Virol. **68:**3879–3887.
29. **Rein, A.** 1982. Interference grouping of murine leukemia viruses: a distinct receptor for the MCF-recombinant viruses in mouse cells. Virology **120:**251–257.
30. **Rio-Hortega, P. D.** 1932. Microglia, p. 482–534. *In* W. Penfield (ed.), Cytology and cellular pathology of the nervous system. Hoeber, New York.
31. **Robertson, M. N., M. Miyazawa, S. Mori, B. Caughey, L. H. Evans, S. F. Hayes, and B. Chesebro.** 1991. Production of monoclonal antibodies reactive with a denatured form of the Friend murine leukemia virus gp70 envelope protein: use in a focal infectivity assay, immunohistochemical studies, electron microscopy and Western blotting. J. Virol. Methods **34:**255–271.
32. **Selmaj, K. W., M. Farooq, W. T. Norton, C. S. Raine, and C. F. Brosnan.** 1990. Proliferation of astrocytes in vitro in response to cytokines. A primary role for tumor necrosis factor. J. Immunol. **144:**129–135.
33. **Sitbon, M., J. Nishio, K. Wehrly, D. Lodmell, and B. Chesebro.** 1985. Use of a focal immunofluorescence assay on live cells for quantitation of retroviruses. Distinction of host-range classes in virus mixtures and biological cloning of dual-tropic murine leukemia viruses. Virology **141:**110–118.
34. **Sitbon, M., B. Sola, L. Evans, J. Nishio, S. F. Hayes, K. Nathanson, C. F. Garon, and B. Chesebro.** 1986. Hemolytic anemia and erythroleukemia, two distinct pathogenic effects of Friend MuLV: mapping of the effects to different regions of the viral genome. Cell **47:**851–859.
35. **Szurek, P. F., P. H. Yuen, J. K. Ball, and P. K. Y. Wong.** 1990. A Val-25-to-Ile substitution in the envelope precursor polyprotein, $gPr80^{env}$, is responsible for the temperature sensitivity, inefficient processing of $gPr80^{env}$, and neurovirulence of *ts*1, a mutant of Moloney murine leukemia virus TB. J. Virol. **64:**467–475.
36. **Tyor, W. R., J. D. Glass, J. W. Griffin, P. S. Becker, J. C. McArthur, L. Bezman, and D. E. Griffin.** 1992. Cytokine expression in the brain during the acquired immunodeficiency syndrome. Ann. Neurol. **31:**349–360.
37. **Wong, P. K.** 1990. Moloney murine leukemia virus temperature-sensitive mutants: a model for retrovirus-induced neurologic disorders. Curr. Top. Microbiol. Immunol. **160:**29–60.
38. **Zachary, J. F., C. J. Knupp, and P. K. Y. Wong.** 1986. Noninflammatory spongiform polioencephalomyelopathy caused by a neurotropic temperature-sensitive mutant of Moloney murine leukemia virus TB. Am. J. Pathol. **124:**457–468.